



# Reverse-bias Leakage Current Mechanisms in Cu/n-type Schottky Junction Using Oxygen Plasma Treatment

Hogyoun Kim<sup>†</sup>

Department of Visual Optics and Convergence Institute of Biomedical Engineering & Biomaterials, Seoul National University of Science and Technology (Seoultech), Seoul 01811, Korea

Received January 25, 2016; Revised February 15, 2016; Accepted February 16, 2016

Temperature dependent reverse-bias current-voltage ( $I$ - $V$ ) characteristics in Cu Schottky contacts to oxygen plasma treated n-InP were investigated. For untreated sample, current transport mechanisms at low and high temperatures were explained by thermionic emission (TE) and TE combined with barrier lowering, respectively. For plasma treated sample, experimental  $I$ - $V$  data were explained by TE or TE combined with barrier lowering models at low and high temperatures. However, the current transport was explained by a thermionic field emission (TFE) model at intermediate temperatures. From X-ray photoemission spectroscopy (XPS) measurements, phosphorus vacancies (VP) were suggested to be generated after oxygen plasma treatment.  $V_p$  possibly involves defects contributing to the current transport at intermediate temperatures. Therefore, minimizing the generation of these defects after oxygen plasma treatment is required to reduce the reverse-bias leakage current.

**Keywords:** InP, Current transport mechanisms, Phosphorous vacancies

## 1. INTRODUCTION

Indium phosphide (InP) has been a promising material in the field of electronic devices such as laser diodes, photo-detectors, solar cells, high electron mobility transistors (HEMTs), high speed metal-insulator-semiconductor field effect transistors (MISFETs), microwave sources and amplifiers due to its direct band gap, good temperature stability, high frequency response and high electron saturation velocity ( $2.5 \times 10^7$  cm/s) [1-5]. In order to realize such devices the electrical properties of metal-semiconductor (MS) interface must be thoroughly understood. The progress in InP devices has been limited by low Schottky barrier height, poor stability and large reverse leakage current [6,7]. Therefore, there has been strong attention in developing thermally-stable rectifying contacts to InP with high barrier height and low leakage current [8,9].

The electrical and structural properties of the Schottky con-

tacts to undoped (unintentionally n-type doped) and intentionally n-type InP have been investigated by several research groups. Assuming that Fermi-level pinning is caused by a high density of surface states, passivation technology has been employed to reduce the density of surface states [6,10,11]. For example, Jeng *et al.* reported the barrier height as high as 0.95 eV in Ag/n-InP (S-doped InP with a carrier concentration of  $5 \times 10^{17}$  cm<sup>-3</sup>) Schottky diode using phosphorous sulfide/ammonia sulfide [ $P_{2S_5}/(NH_4)_2S_x$ ] solution [10]. Modulation of the effective barrier height has been attempted by inserting an insulator or organic layer between the metal and the semiconductor layers [12,13]. For example, Soylu *et al.* investigated the effects of thermal annealing on Au/Pyronine-B/n-InP (S-doped InP with a carrier concentration of  $1.2 \times 10^{16}$  cm<sup>-3</sup>) Schottky structures, and showed that the diode parameters depended on the annealing temperature [13]. The effect of thermal annealing on the electrical properties of InP Schottky junction has also been investigated; Reddy *et al.* determined the effects of rapid thermal annealing on the electrical and structural properties of Pd/Au Schottky contacts to n-InP (undoped InP with a carrier concentration of  $4.5 \times 10^{15}$  cm<sup>-3</sup>) and reported that the formation of indium phases at the interface increasing Schottky barrier height at 400 °C [14]. Janardhanam *et al.* fabricated Mo/n-InP (undoped

<sup>†</sup> Author to whom all correspondence should be addressed:

E-mail: [hogyoungkim@gmail.com](mailto:hogyoungkim@gmail.com)

Copyright ©2016 KIEEME. All rights reserved.

This is an open-access article distributed under the terms of the Creative Commons Attribution Non-Commercial License (<http://creativecommons.org/licenses/by-nc/3.0>) which permits unrestricted noncommercial use, distribution, and reproduction in any medium, provided the original work is properly cited.

InP with a carrier concentration of  $5 \times 10^{15} \text{ cm}^{-3}$  Schottky diode and investigated the electrical, structural and surface morphological properties as a function of annealing temperature. The decrease in barrier height after annealing at  $500^\circ\text{C}$  was reported to be due to the formation of phosphide phases at the interface [15].

The dominant process that determines the electron transport in Schottky junction when a bias voltage is applied to the junction can be understood by considering various transport models. In addition, the analysis of temperature dependent current-voltage ( $I$ - $V$ ) characteristics is a method to investigate the physical mechanisms associated with the reverse-bias leakage current in the material. Miller *et al.* presented temperature-dependent  $I$ - $V$  measurements of Schottky diodes fabricated on GaN grown by molecular beam epitaxy, [16] suggesting two dominant leakage current mechanisms [16]. Ueda *et al.* investigated  $I$ - $V$  characteristics of Cu/diamond Schottky diodes at high-temperature and high-voltage characteristics and found the dominant transport mechanisms under reverse-bias condition [17]. Oxygen plasma treatment known as an effective, economic and environmentally safe method is widely used during the device fabrication process to clean the semiconductor surface and to prepare for further processing. Through such cleaning processes, residual organics, metallic contaminants and native oxides from the semiconductor surface should be removed completely during the fabrication. In this respect, investigation of the reverse-bias leakage current for oxygen plasma treated InP is meaningful to improve the device performance. Here, we explore comparatively the current transport mechanism of Cu/n-InP Schottky contacts under reverse-bias conditions with and without oxygen plasma treatment.

## 2. EXPERIMENTAL

As a starting material, single side polished undoped (unintentionally n-type doped) InP (100) wafer (thickness:  $350 \mu\text{m}$ ), having a carrier concentration of  $\sim 1 \times 10^{16} \text{ cm}^{-3}$  was used. The wafer was first cut into small pieces and some of these pieces were subjected to oxygen plasma treatment on the polished side. Oxygen plasma was produced with a plasma power of  $250 \text{ W}$  at the atmospheric pressure with an oxygen flow rate of  $40 \text{ sccm}$  and an Ar flow rate of  $8 \text{ sccm}$ . After solvent cleaning, Cu Schottky contacts with thicknesses of  $100 \text{ nm}$  were deposited by using radio-frequency (RF) magnetron sputtering through a shadow mask onto the polished side for all the samples. For ohmic contacts,  $150 \text{ nm}$  thick Al metal was deposited over the entire back surface of the samples. Current-voltage ( $I$ - $V$ ) measurements were carried out in the temperature range of  $100$ - $300 \text{ K}$  with a Keithley 4200 SCS and a cryogenic probe station (Janis ST-500). X-ray photoelectron spectroscopy (XPS) measurements were carried out using a monochromatic Mg  $K\alpha$  x-ray source to observe the formation mechanism of Cu/n-InP contact.

## 3. RESULTS AND DISCUSSION

Figure 1 shows the typical linear  $I$ - $V$  characteristics measured in temperatures of  $100 \text{ K}$  -  $300 \text{ K}$ , showing rectifying characteristics. With increasing temperature, the forward bias current values also increased for both samples. As shown in the inset of Fig. 1(b), the reverse-bias current values are similar at  $100 \text{ K}$ ,  $260 \text{ K}$ , and  $300 \text{ K}$ , but these are higher for plasma treated sample at other temperatures ( $140 \text{ K}$ ,  $180 \text{ K}$ , and  $220 \text{ K}$ ). Different transport mechanisms are indicated at intermediate temperatures.

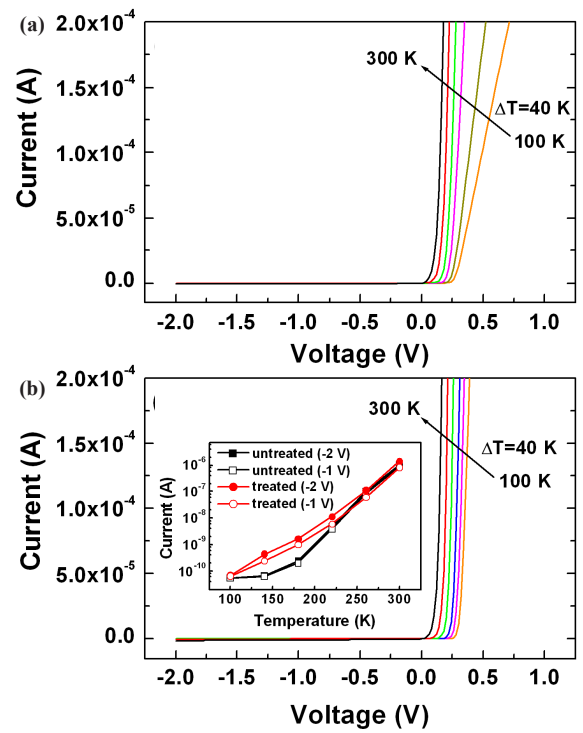


Fig. 1. Linear current-voltage ( $I$ - $V$ ) characteristics for (a) untreated and (b) plasma treated samples measured in the temperature range of  $100\text{K}$ - $300\text{K}$ . The inset in (b) depicts the reverse bias current values at different temperatures.

The reverse current,  $I_R$  were analyzed by using various models such as TE [18], TE combined with barrier lowering (BL) [18], TFE [19], which are expressed by following equations

$$I_R^{TE} = AA^{**}T^2 \exp(-q\phi_B^{TE} / kT) \quad (1)$$

$$I_R^{TE+BL} = AA^{**}T^2 \exp(-q\phi_B^{TE} / kT) \exp(q\sqrt{qE} / (4\pi\epsilon_s) / kT) \quad (2)$$

$$\text{where } E = \sqrt{2qN_D / \epsilon_s (V + V_0 - kT / q)}$$

$$I_R^{TFE} = I_S^{TFE} \exp\left(\frac{V_R}{kT} - \frac{V_R}{E_{00} \coth(E_{00} / kT)}\right) \quad (3)$$

and

$$I_S^{TFE} = \frac{AA^{**}T\sqrt{\pi E_{00}}}{k} \sqrt{(V_R - V_0) + \frac{\phi_B^{TFE}}{\coth^2(E_{00} / kT)}} \times \exp\left(-\frac{\phi_B^{TFE}}{E_{00} \coth(E_{00} / kT)}\right) \quad (4)$$

where  $V_R$  is the reverse bias,  $A^{**}$  is the Richardson constant,  $V_0 = kT / q \ln(N_C / N_D)$  is the potential difference between conduction band and Fermi level,  $E_{00} = (q\hbar / 2)(N_d / m_e \epsilon_s)^{1/2}$  is the characteristic energy related to the tunneling probability, and  $\phi_B^{TE}$  and  $\phi_B^{TFE}$  are the barrier heights for TE and TFE models, respectively. Fitting to experimental reverse-bias  $I$ - $V$  data with

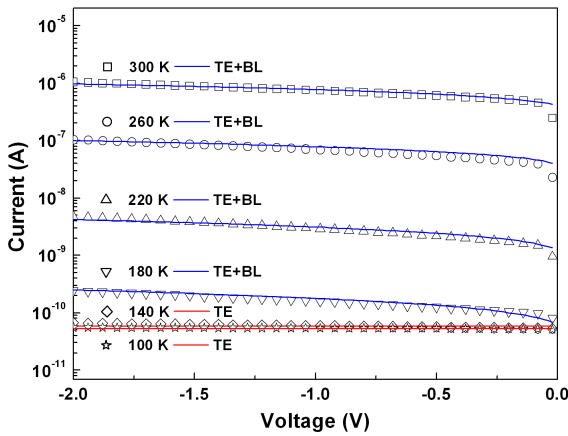


Fig. 2. Fitting results of the reverse-bias current-voltage (*I-V*) characteristics for untreated sample. The lines represent theoretical current components estimated by the thermionic emission (TE) and TE combined with barrier lowering (BL).

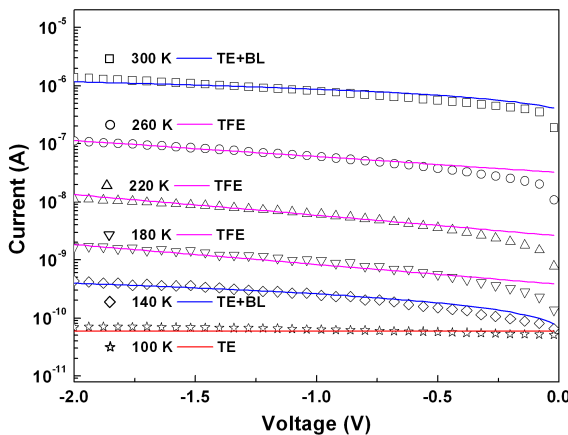


Fig. 3. Fitting results of the reverse-bias current-voltage (*I-V*) characteristics for oxygen plasma treated sample. The lines represent theoretical current components estimated by the thermionic emission (TE), the TE combined with barrier lowering (BL) and the thermionic field emission (TFE) model.

theoretical *I-V* curves was carried out for each sample considering  $\phi_B^{TE}$ ,  $E_{00}$  and  $\phi_B^{TFE}$  as fitting parameters. Figure 2 shows comparison between the experimental and the fitted *I-V* curves for untreated sample. At low temperatures (100 K and 140 K), the experimental data fitted well with the TE model. The fitting values of barrier height were 0.240 eV and 0.343 eV at 100 K and 140 K, respectively. With further increase in temperature, the experimental data were explained by TE combined with a barrier lowering model. The fitting values of barrier height were 0.460 eV, 0.512 eV, 0.533 eV, and 0.562 eV at 180 K, 220 K, 260 K, and 300 K, respectively.

Figure 3 shows comparison between the experimental and the fitted *I-V* curves for plasma treated sample. At 100 K, the experimental data were fitted well by TE model. The fitting value of barrier height was 0.239 eV. At 140 K, the experimental data were fitted well with TE combined with the barrier lowering model with the fitting value of barrier height as 0.353 eV. With further temperature increase, the experimental data were explained by a TFE model instead of TE combined with a barrier lowering model. The fitting values of  $E_{00}$  were calculated to be 2.5 meV,

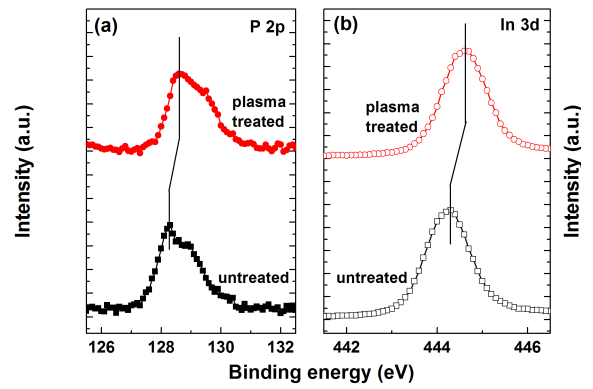


Fig. 4. X-ray photoemission spectroscopy (XPS) spectra of (a) P 2p and (b) In 3d core levels for both samples.

3.3 meV, and 4.0 meV at 180 K, 220 K, and 260 K, respectively. These values correspond to the apparent carrier concentration of  $1.4 \times 10^{16} \text{ cm}^{-3}$ ,  $2.5 \times 10^{16} \text{ cm}^{-3}$  and  $3.7 \times 10^{16} \text{ cm}^{-3}$  at 180 K, 220 K and 260 K, respectively. In addition, these values are larger than the values of  $5.0 \times 10^{15} \text{ cm}^{-3} \sim 1.0 \times 10^{16} \text{ cm}^{-3}$  determined from capacitance-voltage (*C-V*) measurements. Here, *C-V* data for the untreated and plasma treated samples were measured at 300 K using a Keithley 4200 SCS. Because interface states cannot follow an AC signal at sufficiently high frequencies ( $f \geq 1 \text{ MHz}$ ) [20], characterization took place at 1 MHz to eliminate the contribution of these states. The carrier concentrations were extracted from the slopes of plots of  $A^2/C^2$  as a function of reverse bias  $V_R$ , where  $A$  is the diode area. The interface states near the surface were generated for plasma treated sample, which enhanced the tunneling probability and thus were explained by TFE model. At 300 K, the experimental data were fitted well by TE combined with barrier lowering model with the fitting value of barrier height as 0.569 eV. Considering that the current transport mechanisms were explained by TE combined with barrier lowering model at low and high temperatures and by TFE model at intermediate temperatures, the activation of interface states generated by oxygen plasma might be dependent on the temperature.

In order to investigate the contact formation mechanisms in more detail, XPS measurements were performed after depositing 10 nm thick Cu metal layers on both untreated and plasma treated InP samples. As shown in Figure 4, the peak positions of P 2p and In 3d core levels shifted to higher binding energy after oxygen plasma treatment, which indicates the surface Fermi energy movement toward the conduction band edge, resulting in a decrease in the upward surface band bending. The decreased surface band bending could lead to decreased barrier height [21]. The average Schottky barrier height from *I-V* measurements at room temperature for 8~10 Schottky diodes were found to be  $0.469 (\pm 0.003) \text{ eV}$  and  $0.482 (\pm 0.010) \text{ eV}$ , respectively, for untreated and plasma treated samples. Although, the XPS spectra indicated that the barrier height would decrease after plasma treatment, the results from *I-V* indicated the effect of oxygen plasma treatment on the barrier height is negligible.

Further information on the interfacial reaction between Cu metal layer and n-InP film was obtained from the XPS depth profiles as shown in Fig. 5. The atomic percents of O atoms present on the InP surface are similar, implying that O atoms after plasma treatment did not stay near the InP surface. Compared to untreated sample, the atomic percents of In atoms are higher and those of Cu and P atoms are lower for plasma treated sam-

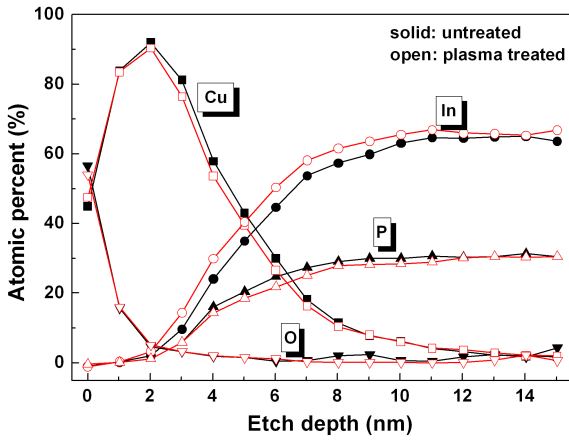


Fig. 5. X-ray photoemission spectroscopy (XPS) depth profiles for both samples.

Table 1. Fitting parameters for theoretical  $I$ - $V$  curves.

Temp.(K)	untreated			plasma treated		
	(eV)	(eV)	(meV)	(eV)	(eV)	(meV)
100	0.240	-	-	0.239	-	-
140	0.343	-	-	0.353	-	-
180	0.460	-	-	-	0.458	2.5
220	0.512	-	-	-	0.526	3.3
260	0.533	-	-	-	0.565	4.0
300	0.562	-	-	0.569	-	-

ple. Both samples show that In and P atoms out-diffused into Cu metal layer, resulting in the formation of Cu-In and Cu-P interfacial phases at the interface. Figure 5 also shows that the relative P/In ratio became smaller after plasma treatment, suggesting the presence of phosphorous vacancies.

Using deep level transient spectroscopy (DLTS) measurements, Ahaitouf *et al.* observed the distribution of interface states with the peak at  $\sim 220$  K with the activation energy lower than 0.2 eV [22]. Based on these results, the origin of interface states was attributed to phosphorus vacancies ( $V_p$ ) or indium vacancies ( $V_{in}$ ). This trap was also attributed to interface states due to phosphorus vacancies occupied by oxygen after surface treatment [22,23]. Meanwhile, Janardhanam *et al.* observed the deep trap with the peak at  $\sim 220$  K (activation energy of 0.18 eV) in Pd/n-InP Schottky diodes after annealing at  $400^\circ\text{C}$  and also associated the peak with  $V_{in}V_p$  divacancy defects [24]. Using a positron-lifetime study, Shan *et al.* found that a large amount of  $V_p$  vacancies form after PP atoms migrate to interstitial sites and then  $V_p$  vacancies which are in the vicinity of indium vacancies could combine to form  $V_{in}V_p$  divacancies. [25]. Although the analysis on XPS results in this work showed that P/In atomic ratio decreased after oxygen plasma treatment, we cannot rule out the possibility that both  $V_{in}$  and  $V_p$  might be generated after oxygen plasma treatment. Then, the interface states generated from oxygen plasma treatment could be associated to the  $V_{in}V_p$  divacancies, and these defects may contribute to the total current transport at intermediate temperatures (180 K  $\sim$  260 K). However, further research should be performed to clarify the exact origin.

## 4. CONCLUSION

Using current-voltage ( $I$ - $V$ ) measurements, the current trans-

port mechanisms of Cu Schottky contacts to oxygen plasma treated n-InP under reverse-bias condition were investigated comparatively. The suitable current transport models for untreated sample has changed from thermionic emission (TE) to TE combined with barrier lowering with increasing the temperature. For plasma treated samples, the experimental data were explained by TE and TE combined with barrier lowering models, respectively, at 100 K and 140 K. At intermediate temperatures, the current transport was explained by thermionic field emission (TFE) model. At 300 K, TE combined with barrier lowering model fitted well with the experimental  $I$ - $V$  data. Probably  $V_p$  involved defects ( $V_{in}V_p$  divacancies) may contribute to the total current transport at intermediate temperatures.

## ACKNOWLEDGMENTS

This study was supported by the Research Program funded by the Seoul National University of Science and Technology (Seoultech).

## REFERENCES

- [1] P. Cova, A. Sing, A. Medina, and R. Masut, *Solid State Electron.* **42**, 477 (1997). [DOI: [http://dx.doi.org/10.1016/S0038-1101\(97\)00250-5](http://dx.doi.org/10.1016/S0038-1101(97)00250-5)]
- [2] H. Zhao H, D. Shahrjerdi, F. Zhu, H. Kim, I. Ok, M. Zhang, J. Yum, S. Nanerjee, and J. Lee, *Electrochem Solid State Lett.* **11**, H233 (2008). [DOI: <http://dx.doi.org/10.1149/1.2938728>]
- [3] Y. Wang, X. Yang, T. He, Y. Gao, H. Demir, X. Sun and H. Sun, *Appl. Phys. Lett.* **102**, 021917 (2013). [DOI: <http://dx.doi.org/10.1063/1.4776702>]
- [4] A. Sing, K. Reinhardt, and W. Anderson, *J. Appl. Phys.* **68**, 3475 (1990). [DOI: <http://dx.doi.org/10.1063/1.346358>]
- [5] K. Hattori, and Y. Torii, *Solid State Electron.* **34**, 527 (1991). [DOI: [http://dx.doi.org/10.1016/0038-1101\(91\)90157-T](http://dx.doi.org/10.1016/0038-1101(91)90157-T)]
- [6] T. Sugino, H. Ito, and J. Shirafuji, *Electron. Lett.* **26**, 1750 (1990). [DOI: <http://dx.doi.org/10.1049/el:19901124>]
- [7] J. Dow, and R. Allen, *J. Vac. Sci. Technol.* **20**, 659 (1982). [DOI: <http://dx.doi.org/10.1116/1.571620>]
- [8] H. Cetin, and E. Ayyildiz, *Semicond. Sci. Technol.* **20**, 625 (2005). [DOI: <http://dx.doi.org/10.1088/0268-1242/20/6/025>]
- [9] L. Chou, K. Hsieh, D. Wohler, and K. Cheng, *J. Appl. Phys.* **84**, 6932 (1998). [DOI: <http://dx.doi.org/10.1063/1.368993>]
- [10] M. Jeng, H. Wang, L. Chang, Y. Cheng, and S. Chou, *J. Appl. Phys.* **86**, 6261 (1999). [DOI: <http://dx.doi.org/10.1063/1.371682>]
- [11] T. Huang, and R. Fang, *Solid State Electron.* **37**, 1461 (1994). [DOI: [http://dx.doi.org/10.1016/0038-1101\(94\)90152-X](http://dx.doi.org/10.1016/0038-1101(94)90152-X)]
- [12] A. Astito, A. Foucaran, G. Bastide, and M. Rouzeyre, *J. Appl. Phys.* **70**, 2584 (1991). [DOI: <http://dx.doi.org/10.1063/1.349366>]
- [13] M. Soyulu, B. Abay, and Y. Onganer, *J. Phys. Chem. Solids* **71**, 1398 (2010). [DOI: <http://dx.doi.org/10.1016/j.jpcs.2010.07.003>]
- [14] M. Reddy, V. Janardhanam, A. Kumar, V. Reddy, and P. Reddy, *Phys. Status Solidi A* **206**, 250 (2009). [DOI: <http://dx.doi.org/10.1002/pssa.200824268>]
- [15] V. Janardhanam, A. Kumar, V. Reddy, and P. Reddy, *Surf. Interface Anal.* **41**, 905 (2009). [DOI: <http://dx.doi.org/10.1002/sia.3114>]
- [16] E. Miller, E. Yu, P. Waltereit, and J. Speck, *Appl. Phys. Lett.* **84**, 535 (2004). [DOI: <http://dx.doi.org/10.1063/1.1644029>]
- [17] K. Ueda, K. Kawamoto, and H. Asano, *Diamond & Related Mater.* **57**, 28 (2015). [DOI: <http://dx.doi.org/10.1016/j.diamond.2015.03.006>]
- [18] S. Sze, *Physics of Semiconductor Devices* (Wiley, New York, 1981).

- [19] F. Padovani, and R. Stratton, *Solid State Electron.* **9**, 695 (1966). [DOI: [http://dx.doi.org/10.1016/0038-1101\(66\)90097-9](http://dx.doi.org/10.1016/0038-1101(66)90097-9)]
- [20] E. Nicollian and J. Brews, *Metal Oxide Semiconductor (MOS) Physics and Technology* (Wiley, New York, 1981).
- [21] C. Jeon, and J. Lee, *Appl. Phys. Lett.* **82**, 4301 (2003). [DOI: <http://dx.doi.org/10.1063/1.1583140>]
- [22] A. Ahaitouf, E. Losson, and A. Bath, *Solid State Electron.* **44**, 515 (2000). [DOI: [http://dx.doi.org/10.1016/0038-1101\(66\)90097-9](http://dx.doi.org/10.1016/0038-1101(66)90097-9)]
- [23] N. Newman, W. Spicer, T. Kendelewicz, and I. Lindau, *J. Vac. Sci. Technol. B* **4**, 931 (1986). [DOI: <http://dx.doi.org/10.1116/1.583494>]
- [24] V. Janardhanam, A. Kumar, V. Reddy, and P. Reddy, *J. Mater. Sci.: Mater. Electron.* **21**, 285 (2010). [DOI: <http://dx.doi.org/10.1007/s10854-009-9906-3>]
- [25] Y. Shan, A. Deng, C. Ling, S. Fung, and C. Ling, *J. Appl. Phys.* **91**, 1998 (2002). [DOI: <http://dx.doi.org/10.1063/1.1428796>]